

Influence of roughness on the behavior of three-dimensional journal bearing based on fluid-structure interaction approach

by Mohammad Tauviqirrahman

Submission date: 19-Jan-2020 10:08AM (UTC+0700)

Submission ID: 1346304577

File name: Tauviqirrahman_JMST_Paper.pdf (2.18M)

Word count: 5537

Character count: 30012

Influence of roughness on the behavior of three-dimensional journal bearing based on fluid-structure interaction approach[†]

Mohammad Tauviquirrahman^{1,*}, Brain Choirul Ichsan¹, Jamari¹ and Muchammad²

¹Laboratory for Engineering Design and Tribology, Department of Mechanical Engineering, Diponegoro University, Semarang, Indonesia

²Laboratory for Surface Technology and Tribology, Faculty of Engineering Technology, Twente University, Enschede, The Netherlands

(Manuscript Received March 29, 2019; Revised July 6, 2019; Accepted August 8, 2019)

Abstract

In present study, a fluid-structure interaction (FSI) approach is proposed for predicting the effects of roughness on the performance of hydrodynamically lubricated three-dimensional (3D) journal bearing, taking mechanical deformation effects. The multi-phase cavitation mass flow conservation model is adopted, in which the phase change boundary condition is allowable. The results show that the mechanical deformation effect on bearing performance has been confirmed to be substantial. When the deformation of the structure is considered in calculating the change of film thickness, the bearings carry less load (i.e. 30-70 % smaller depending on the surface roughness value) as compared to the case in which the deformation is neglected. It is also highlighted that the hydrodynamic pressure and load support decrease with surface roughness.

Keywords: Cavitation; Deformation; Fluid-structure interaction (FSI); Journal bearing; Roughness

1. Introduction

The main goal of this research is to explore the influence of roughness on three-dimensional journal bearing because ideal (perfectly smooth) surfaces are impossible to find in real due to irregularities nature. In the main frame of this nature, many workers [1-4] proposed to investigate the surface roughness influences on the bearing performance.

Gururajan and Prakash [1] have investigated the effect of surface roughness in a narrow porous journal bearing. This work was based on the Christensen's stochastic theory of rough surfaces. The range of operating parameters for which the approximate solution is acceptable from an engineering viewpoint have been determined. Naduvnamani et al. [2] pointed out the considerable effect of the combined effects of couple stresses and the bearing surface roughness on the lubrication performance. It was found that for the longitudinal roughness configuration the effects of couple stresses are more pronounced as compared to the transverse roughness one. In the presence of slip boundary, the effect of the surface roughness on porous finite journal bearing was studied by Kalavathi et al. [3]. They concluded that the pressure and load support increase with surface roughness for the bearing with mixed slip surface. In the context of the bearing operation, the sur-

face roughness effect in transient condition has been investigated in recent work by Cui et al. [4]. In their work, a mixed lubrication model taking into account both asperities contact and hydrodynamic fluid flow was calculated. The transient average film thickness, the transient movement of the journal center, the contact pressure, and the hydrodynamic pressure were examined for different values of surface roughness. It was highlighted that the surface roughness has a significant effect on the characteristics during the initial period of startup.

As a note, the available literature survey mentioned above indicates that the mechanical deformation of structure (i.e. bearing and/or shaft) was neglected. Dealing with the significance of the deformation effect in lubrication, there were few scholars considering mechanical deformation of the shaft/journal as well as the bearing housing in the study of journal bearing performance [5-8]. It is worth to mention the early work of Liu et al. [5] who explored the use of fluid-structure interaction (FSI) to predict the bearing behavior varying kinds of bearing materials and dynamic unbalanced loading of the journal using a commercially available software. It was found that the elastic deformation of the bearing has a significant effect on the performance of the rotor-bearing system. To model cavitation, the simplified phase change boundary condition was assumed. Charitopoulos et al. [6] based on fluid-structure interaction (FSI) approach demonstrated that the stator (pad) deformation generates a pattern similar to the yielded pressure distribution. In their work, however, one-way

*Corresponding author. Tel.: +62 24 7460059, Fax: +62 24 7460059

E-mail address: mohammad.tauviquirrahman@ft.undip.ac.id

[†]Recommended by Associate Editor Tatacipta Dirgantara

© KSME & Springer 2019

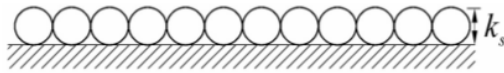


Fig. 1. Schematic representation of uniform sand-grain roughness. Note: K_s is roughness height.

FSI was employed. It should be noted that in one-way FSI technique, the deformation of structure was not used in calculating the change in the film thickness. Other interesting study conducted by Wodtke et al. [7] confirmed that the use of FSI procedure in predicting the bearing performance generates better agreement with the performance obtained with experimental data compared to non-FSI technique. On the other words, the authors suggested to consider the deformation of the structure for predicting the bearing characteristics. In recent publication, Linjamaa et al. [8] showed that the elastic and thermal deformations have a significant effect on bearing performance. In their study, the deformations were predicted using the integrated finite element method, while hydrodynamics were based on the Reynolds equation.

Based on literature survey discussed above, one can find that the studies related to journal bearing system considering the mechanical deformation are rather very-limited. Also, it has been observed from the literature that the cavitation that often occurs in the divergent zone of the journal bearing was not properly modelled. Therefore, to complement the previous findings, in the present work the elastic deformation is taken into account. The main aim of the present study is to investigate the surface roughness effects by a means of fluid-structure interaction (FSI) approach either in one-way FSI or two-way FSI on three-dimensional journal bearing. During the calculation process, the phase change boundary condition is considered to model the cavitation in fluid domain. As a note, most of previously published works the lubricant vaporization was not considered. The inclusion of mass-flow preserving cavitation model as well as mechanical deformation provides a more realistic prediction of the actual operating process of a journal bearing with roughness. Based on our best knowledge, this is the first study combining CFD with a two-way FSI technique to model the elastohydrodynamic (EHD) lubrication within a roughened journal bearing whilst considering multiphase cavitation model.

2. Method

2.1 Roughness model

Once the journal bearing is manufactured, the finishing process may yield different surface roughness levels. In order to investigate the effect of roughness, in this work the roughness is modelled as uniform sand-grain roughness defined by roughness height parameter K_s as shown in Fig. 1. In this approach, the height is assumed constant per surface. For computations, in ANSYS FLUENT® the roughness height K_s must be specified in the surface boundary condition.

As a note, the roughness height K_s is the equivalent sand

grain roughness height, and is not equal to the geometric roughness height of the surface. Therefore, the equivalent sand-grain roughness height must be correlated with the appropriate geometric roughness parameters as measured surface roughness parameters, for instance, R_a (arithmetic average of the roughness profile). According to Adams et al. [9], the correlation between K_s and R_a can be approximated as follows:

$$K_s = 5.863 R_a. \quad (1)$$

Since the correlation as depicted in Eq. (1) has been experimentally verified [9], for all following computations the surface roughness parameter R_a measured by the profilometer can be used as an input to specify the roughness of the bearing surface.

2.2 Basic theory

The steady three-dimensional turbulent Navier-Stokes equations are calculated for the lubricant film flow considering the effects of the body force and inertial force terms. For fluid dynamics studies, the analysis focuses on solving momentum conservation (Eq. (2)) and mass conservation (Eq. (3)) equations. For detailed derivation of these equations, the interested reader is referred to additional Ref. [10].

$$\frac{\partial}{\partial x_i} (\rho u_i u_i) = -\frac{\partial p}{\partial x_i} + \frac{\partial}{\partial x_j} \left[\mu \frac{\partial u_i}{\partial x_j} - \rho \overline{u_i' u_j'} \right] \quad (2)$$

$$\frac{\partial}{\partial x_i} (\rho u_i) = 0. \quad (3)$$

In Eqs. (2) and (3), ρ is the density of the fluid; u_i and u_j are the average velocity components for x, y, z ; p is the static hydrodynamic pressure; μ is the viscosity; u_i' and u_j' are the fluctuation velocities; $-\rho \overline{u_i' u_j'}$ is the Reynolds stress; and $i, j = 1, 2, 3$ (x, y, z). In the present work, the Reynolds stress is solved by the standards k and ϵ [10, 11].

As is known, during the operation of the journal bearing, the cavitation of lubricant often occurs, especially in the divergent zone. Therefore, for all, the cavitation phenomenon in the computational fluid domain is modelled by using a phase change boundary condition, which assumes that cavitation results from the pressure change in fluid domain. In this way, the growth of gas bubbles often accompanies the cavitation process. The cavitation and fluid models are coupled through momentum and single set of density equations for the mixture. The validity of this method has been demonstrated in previously published works [12–16].

In ANSYS FLUENT®, there are three available cavitation models: Schneer and Sauer model, Zwart-Gelber-Belamri model and Singhal et al. model [11]. In this study, the Zwart-Gelber-Belamri is employed due to their capability (less sensitive to mesh density, robust and converge quickly [11]).

In cavitation, the liquid-vapor mass transfer (evaporation

and condensation) is governed by the vapor transport equation [11]:

$$\frac{\partial}{\partial t}(\alpha_v \rho_v) + \nabla \cdot (\alpha_v \rho_v \mathbf{v}) = R_g - R_c \quad (4)$$

where α_v is vapor volume fraction and ρ_v is vapor density. R_g and R_c account for the mass transfer between the liquid and vapor phases in cavitation. For Zwart-Gelber-Belamri model assuming that all the bubbles have the same size in a system, the final form of the cavitation is as follows [17]:

$$p \leq p_v, \quad R_g = F_{\text{evap}} \frac{3\alpha_{\text{mic}}(1-\alpha_v)\rho_v}{R_b} \sqrt{\frac{2}{3}} \frac{P_v - P}{\rho_l} \quad (5)$$

$$p \geq p_v, \quad R_c = F_{\text{cond}} \frac{3\alpha_v \rho_v}{R_b} \sqrt{\frac{2}{3}} \frac{P - P_v}{\rho_l} \quad (6)$$

where F_{evap} = evaporation coefficient = 50, F_{cond} = condensation coefficient = 0.01, R_b = bubble radius = 10^{-6} m, α_{mic} = nucleation site volume fraction = 5×10^{-4} , ρ_l = liquid density and p_v = vapor pressure.

Once the hydrodynamic pressure is predicted through Eq. (2), the load support of lubrication W can be calculated by integrating the pressure p over the journal surface as follows:

$$W = \iint_A p r d\theta dz \quad (7)$$

where θ indicates the circumferential angle from the maximum film thickness and r expresses the shaft radius.

Fluid-structure interaction (FSI) is coupling finite element method (FEM) software environment and computational fluid dynamic (CFD) software environment. For FSI (fluid-structure interaction) analysis in this work, the deformation of shaft journal and the housing is calculated. For solid dynamics problems, the balance equation governing the solid domain derived from Newton's second law reads:

$$\rho_s \ddot{\mathbf{d}}_s = \text{div} \boldsymbol{\sigma}_s + \mathbf{F}_s \quad (8)$$

where subscript s refers to solid designation, ρ_s is the density, $\ddot{\mathbf{d}}_s$ denotes the local acceleration vector, $\boldsymbol{\sigma}_s$ indicates the stress tensor and \mathbf{F}_s expresses the body force vector.

During the solution process, the finite volume method is used to solve the lubricant performance through FLUENT module of the ANSYS software, while bearing's mechanical performances are calculated with the finite element approach employed through the transient structural module of this version. In ANSYS, the system coupling may allow the execution of the data exchange in corresponding iteration stagger between fluid and solid analysis.

In this research, the fluid-shaft and fluid-housing interfaces are considered as coupling walls. Two-types of FSI approach (one-way and two-way FSI) is compared in terms of hydrody-

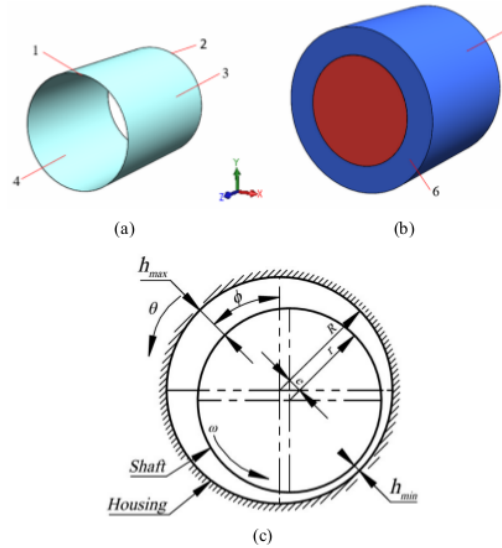


Fig. 2. Configuration of lubricated journal bearing: (a) Fluid domain (lubricant film); (b) solid domain (bearing and shaft); (c) front view of bearing-shaft (1. Pressure inlet, 2. Pressure outlet, 3. Bearing interface, 4. Shaft interface, 5. Outside of housing, 6. Wall of housing. Note: h_{max} is maximum film thickness; h_{min} is minimum film thickness; e is eccentric distance; r is shaft radius; R is inner radius of the bearing; θ is circumferential angle from the maximum film thickness; ϕ is attitude angle; ω is angular velocity).

namic pressure, and load support. As a note, for one-way FSI the deformation of the structure is not considered in calculating the change of film thickness, while for two-way FSI, the deformed geometry is used to solve for the flow field and thus the last one may obtain more realistic behavior of bearing.

2.3 Computational model

The schematic representation of journal bearing is shown in Fig. 2. The bearing represented in Fig. 2 has the following dimensions: The total bearing length $L = 133$ mm, the shaft radius $r = 50$ mm, the housing radius $R = 50.145$ mm, the eccentricity ratio $\varepsilon = 0.61$, and the thickness of housing structure $H_r = 50$ mm. The elastic modulus E and Poisson ratio ν for the bearing with lubricant viscosity μ of 0.0127 Pa.s are 200 GPa and 0.3, respectively. The angular velocity of shaft ω is 48.1 rad/s.

For all following computations, the surface roughness is applied on both the stator and rotor surfaces. In this study, the level of surface roughness (R_a in this study) is varied from 0 (perfectly smooth) to 12.5 μm . As is known, one of process for manufacturing bearing is grinding. According to JIS B 0601-2001, the surface roughness due to grinding process can be categorized as precision ($R_a = 0.1\text{--}0.2 \mu\text{m}$), fine ($R_a = 0.4\text{--}0.8 \mu\text{m}$), medium ($R_a = 1.6\text{--}6.3 \mu\text{m}$), and rough ($R_a = 12.5\text{--}100 \mu\text{m}$). Therefore, in the present work, four classes of surface

roughness, that is, $R_a = 0.1 \mu\text{m}$ (precision), $0.4 \mu\text{m}$ (fine), $1.6 \mu\text{m}$ (medium), and $12.5 \mu\text{m}$ (rough) will be chosen in terms of lubrication performance for following computations.

2.4 Boundary condition

At the bearing as well as journal interfaces, the no-slip boundary conditions are assumed. It means that at the inner surface, the fluid moves with the same velocity as the angular velocity of the shaft. At the outer surface of the fluid domain, the fluid velocity equals to zero. On two sides of the three-dimensional fluid domain, the boundary conditions are set as “pressure inlet” and “pressure outlet”, respectively with relative pressure at zero Pascal (see Fig. 2). At this condition, the volume fraction of the lubricant film is set to one.

In the present study, the governing equations for fluid domain are discretized by finite volume method, which has been employed by ANSYS FLUENT® as commercial CFD software package. In order to obtain an accurate pressure, the SIMPLE algorithm is chosen in the velocity-pressure coupling. For the momentum equations, a second-order upwind discretization scheme is employed whilst for the volume fraction equation, the QUICK discretization scheme is chosen and the others are default. The computational parameters of the fluid domain include lubrication performance parameters such as the hydrodynamic pressure and load support (Eq. (7)).

In this research, the structure model is constructed in ANSYS Design modeler. For all following computations, as seen in Fig. 2, the bearing outer surface is fixed, whilst the inside surface of the bearing housing is set as fluid-solid interface.

2.5 Mesh generation

In the present study, the bearing housing as well as the lubricant film is meshed with the hexahedral element for creating the uniform mesh and enhancing the computation efficiency and precision. Mesh convergence test has been performed to determine an appropriate mesh size in order to achieve the independent mesh. The total number of the elements for the lubricant and the meshed bearing is 1292200 and 145395, respectively. For flow analysis the dynamic mesh technique is employed in ANSYS to model the change in thickness of fluid domain.

3. Results and discussion

3.1 Validation

In order to validate the multi-phase cavitation model with the phase change boundary condition and the developed solution control of numerical approach, a full oil film as well as the mechanical structure of the three-dimensional (finite length) journal bearing is modeled in ANSYS Workbench. As a note, for one-way FSI analysis, the system coupling is not used, while for two-way FSI, the interaction of ANSYS

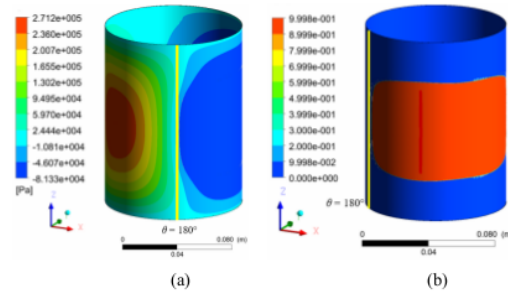


Fig. 3. (a) Nodal hydrodynamic pressure distribution; (b) volume fraction of lubricant vapor. The results are evaluated at the ideal (perfectly smooth) surface ($R_a = 0$). Note: θ is circumferential angle.

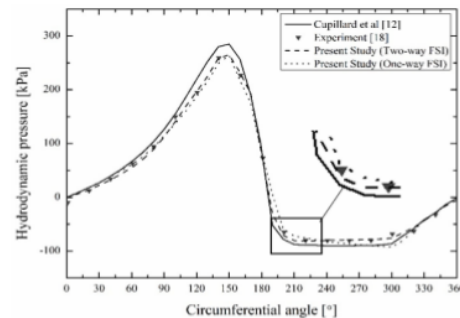


Fig. 4. Numerical and experimental pressure distributions. The “present study” curves are evaluated at $z/L = 0.1$ with the reference z coordinate at the center-line of the bearing as described in Ref. [12]. The results are evaluated at the perfectly smooth surface ($R_a = 0$).

FLUENT for fluid flow analysis and “transient structural” modul for mechanical structure analysis is conducted by system coupling. In this way, some most significant hydrodynamic lubrication performances are calculated.

The parameters of the model for validation purpose are as follows: The radius of journal r is 50 mm, the length of the bearing L is 133 mm, the radial clearance c is 0.145 mm, the angular velocity of the journal ω is 48.1 rad/s, and the eccentricity ratio ε is 0.61. For lubricant properties, the dynamic viscosity μ used is 0.0127 Pa.s, and the density of lubricant ρ is 840 kg/m³. For validation of multi-cavitation model studied here, the vaporization pressure used is 20 kPa which corresponds to a subambient pressure. The dynamic viscosity of lubricant vapor is set to 2×10^{-5} Pa.s and its density to 1.2 kg/m³. It should be noted that the geometry used for validation in this work has identical dimensions to that in CFD model of Cupillard et al. [12] and experimental work of Jakobsson and Floberg [18].

The contours of nodal hydrodynamic pressure profile and volume fraction of lubricant vapor are shown in Figs. 3(a) and (b), respectively, while the comparison result of the pressure distribution between present study (one-way FSI and two-way FSI), CFD simulation [12], and experiment [18] is reflected in

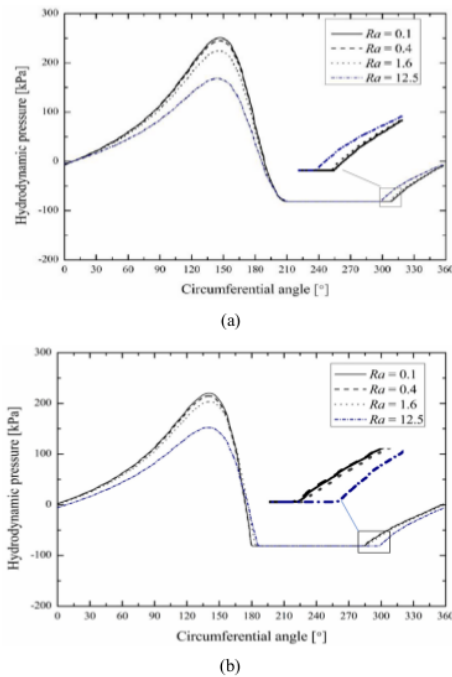


Fig. 5. Influence of surface roughness on hydrodynamic pressure profile based on (a) one-way FSI approach; (b) two-way FSI approach.

As can be observed in Fig. 4, the hydrodynamic pressure distributions predicted by the present approach (one-way FSI and two-way FSI) are in a good agreement with the experimental and other numerical works including the cavitation area with a constant pressure. As a note, the cavitation model used in Ref. [12] is based on the Rayleigh-Plesset model, that is, a multi-phase flow model in which lubricant vapor is generated when hydrodynamic pressure falls below the saturation pressure p_{sat} . In the present study, as mentioned in the previous section, the multi-phase cavitation model of Zwart, Gelber and Belamri [17] is considered here, in which there are some equations of growth and collapse of air bubbles generated in the cavitation zone. The phase change condition and the negative pressure can be observed in divergent zone as illustrated in Fig. 3. Moreover, the feasibility of using two-way FSI approach (in which the deformation of the structure is considered) to predict the lubrication performance of bearing is checked as well. In terms of load support, compared to that in experimental work [18], the relative error is 0.3 and 0.1 percent, respectively, for one-way and two-way FSI method. Generally speaking, the multi-cavitation model as well as the simulation method by considering the deformation of the structure employed here is more suitable to predict the actual working condition of lubricated journal bearing. Besides, based on Fig. 4, the two-way coupling method generates results that well reflect the lubrication behavior of the journal bearing.

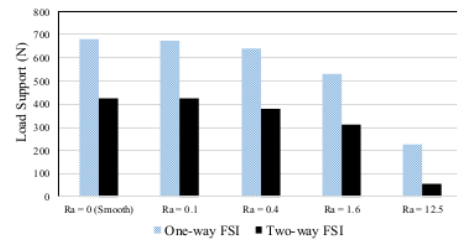


Fig. 6. Comparison of predicted load support between one-way FSI and two-way FSI techniques for different surface roughness values.

3.2 Effect of surface roughness

As evident from the available Refs. [1–4], the surface roughness influences the formation of a lubricant film thickness and thus the hydrodynamic pressure characteristic. In the present study, numerical analysis has been carried out to study the combined effects of surface roughness and mechanical deformation on the lubrication performance (i.e. pressure, load support and volume fraction of lubricant vapor).

The influence of surface roughness on the pressure and load support is shown in Figs. 5 and 6, respectively. Fig. 5 shows that the distribution of hydrodynamic pressure over the surface is strongly affected by the surface roughness regardless of whether the deformation is considered or not. The higher the surface roughness level, the lower the pressure profile as well as the peak pressure. As a consequence, it leads to the decrease in load support as indicated in Fig. 6. In the case of one-way FSI, for example, compared to ideal (perfectly smooth, $R_a = 0$) journal bearing, the load support for roughened bearing reduces up to 1.53 %, 6.37 %, 22.49 % and 67.14 %, respectively, for $R_a = 0.1$, $R_a = 0.4$, $R_a = 1.6$ and $R_a = 12.5$. In the case of which the deformation is included, the decrease in load support becomes larger for all values of surface roughness compared to that of which the deformation effect is excluded. For “rough” surface, the deterioration of the load support up to 86.85 % is observed. From the engineering point of view, these results indicate that the finishing process for creating the desired surface roughness level of contacting surfaces should be well performed in order to prevent the manufacturing errors and achieve the best lubrication performance.

With respect to the cavitation region, based on Fig. 7, it can be underlined that based on the simulation results both for one-way FSI and two-way FSI cases, the distribution of the lubricant vapor does not change very much with the increase in surface roughness. However, for “rough” surface (i.e. R_a of 12.5 μm in this case), the one-way FSI technique gives the smaller area of the lubricant vapor. This trend strengthens the previous result in terms of the length of the cavitation region as observed in Fig. 5(a). Contradictive result is observed when the mechanical deformation is taken into account (i.e. two-way FSI); for “rough” surface the slightly larger distribution of the lubricant vapor is highlighted. The plausible reason for

this is that, for surface with high roughness level, the amount of vapor bubble along the divergent area is increased by the presence of deformed surface asperities and thus more gas bubble is trapped in asperities. It leads to the increase in the vapor volume fraction in the fluid, leading the hydrodynamic pressure value in the remaining lubricant in the convergent area to decrease as well as its peak pressure value.

3.3 Effect of deformation (one-way vs two-way FSI)

In this section, the significance of the inclusion of the deformation effect in lubrication analysis is performed in terms of hydrodynamic pressure and load support through fluid-structure interaction (FSI) technique. For one-way FSI calculation, only the lubricant pressure acting at the structure is transferred to the structure solver. For two-way FSI prediction, the deformation of the structure is also transferred to the fluid solver. In this way, the deformed surface of lubricated contacts will make an updating the film thickness.

Fig. 5 as reflected in the previous section gives the comparison of the hydrodynamic pressure distribution of lubricated contact for two cases: One-way FSI versus two-way FSI for different surface roughness levels. It can be seen from Fig. 5 that one-way FSI method generates the slightly higher result in terms of hydrodynamic pressure and load support compared to two-way FSI one. From the physical point of view, it indicates that the mechanical deformation of bearing gives a significant role in altering the lubrication behavior. When the surface deforms due to hydrodynamic pressure, the change of the film thickness in bearing occurs, and as a consequence the flow field will change. As depicted in Fig. 6, for all roughened bearing, the difference in the predicted load support between one-way and two-way FSI techniques is quite significant, i.e. 30–70 % depend on the surface roughness value.

By comparing two conditions, i.e. one-way and two-way FSI as displayed in Figs. 5(a) and (b), another interesting result is observed, that is, when the two-way FSI is employed, the cavitation zone becomes quite larger. The most possible explanation is that when the deformation of the structure occurs, the film thickness changes. Reminding that the lubricant supply is constant during the bearing operation, the deformed geometry may become a trigger to the change in hydrodynamic pressure values, and finally it leads the phase change in wider area. For detail, dealing with this physical phenomenon, the contours of volume fraction of lubricant vapor-phase are presented in Fig. 7 for different roughness values as shown in the previous section. It can be observed that for all cases the vapor volume fraction mostly occupies the divergent area that generates gas. Specifically, for two-way FSI calculation the distribution of volume fraction of lubricant vapor is larger than that for one-way FSI for all cases. When the elastic deformation exists both in housing and shaft of the bearing system, the clearance value between the housing and shaft increases leading to the change in film thickness. As a consequence, more lubricant will fill in the area diminishing the peak hydrody-

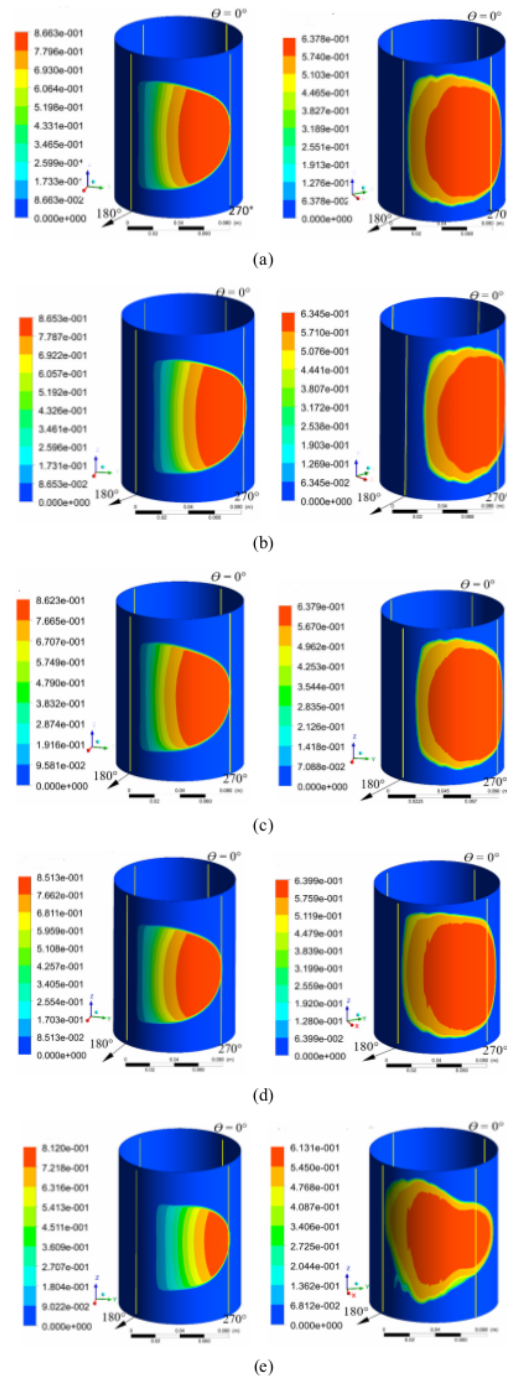


Fig. 7. Comparison of contour of volume fraction for vapor phase between one-way FSI (left) and two-way FSI (right) in the case of (a) perfectly smooth surface ($R_a = 0 \mu\text{m}$); (b) $R_a = 0.1 \mu\text{m}$; (c) $R_a = 0.4 \mu\text{m}$; (d) $R_a = 1.6 \mu\text{m}$; (e) $R_a = 12.5 \mu\text{m}$. Note: θ is circumferential angle.

Table 1. Maximum deformation at different roughness values.

Surface roughness (μm)	Maximum deformation (μm)
0	0.26
0.1	0.26
0.4	0.26
1.6	0.24
12.5	0.19

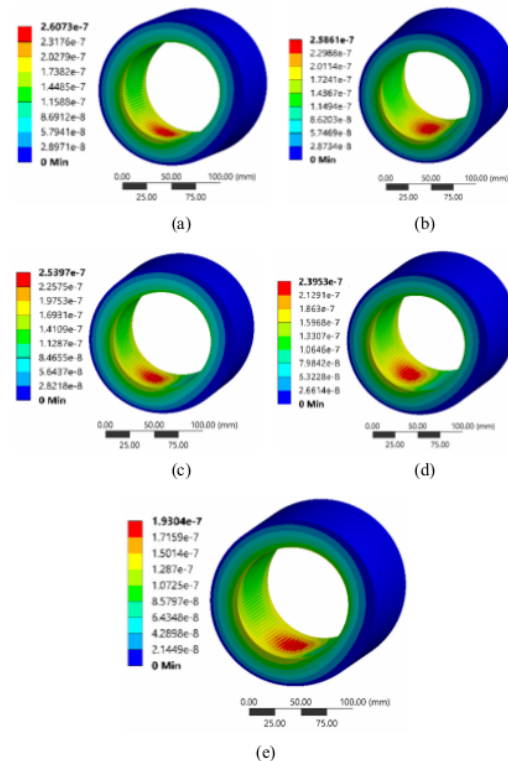


Fig. 8. Contour of bearing deformation (in mm) for the case of (a) perfectly smooth surface ($R_a = 0 \mu\text{m}$); (b) $R_a = 0.1 \mu\text{m}$; (c) $R_a = 0.4 \mu\text{m}$; (d) $R_a = 1.6 \mu\text{m}$; (e) $R_a = 12.5 \mu\text{m}$.

dynamic pressure generated. This is also the reason why the load support is reduced when the deformation effect is taken into account. Overall, it indicates that in order to obtain the closer result to physical observation, the deformation of the structure should be included in the analysis, which means that two-way FSI should be employed.

In order to describe the mechanical performance, the deformation contours of the bearing are depicted in Fig. 8 for different surface roughness values. Two specific features can be found based on Fig. 8. Firstly, for all cases studied here the maximum deformation appears at the convergent region, especially at the position of circumferential angle θ of 145° , which is caused by the high hydrodynamic pressure at the

same location.

Secondly, it is easy to observe that the variation in the surface roughness little affects the deformation value, which implies that the surface roughness effect reflects mainly in altering the tribological performance for the bearing, instead of the mechanical performance. For detail, Table 1 summarizes the maximum deformation of the bearing structure for different surface roughness values.

Based on Table 1, it is interesting to compare the values of the computed deformation with the minimum film thickness. In this study, it is found that the minimum film thickness to maximum deformation ratio ranges from about 200 to 300 depend on the surface roughness level. However, relatively small deformation has been proven to alter the lubrication performance and lead to the deterioration of the predicted load support. From this result, again, it is advisable to consider the effect of mechanical deformation in the bearing analysis.

4. Conclusions

The effect of surface roughness on the performance of three-dimensional journal bearing considering mechanical deformation was studied using fluid-structure-interaction (FSI) method. One-way FSI and two-way FSI methods were compared in terms of hydrodynamic pressure and load support. The investigations revealed that the pressure distribution and load support decrease with the increase in roughness. In addition, it was concluded that the deformation of the solid structure clearly affects the flow pattern and thus it cannot be ignored in lubrication analysis for obtaining more accurate result of bearing performances.

Acknowledgments

This research is fully supported by RPI-BT (Research Publication International-High Reputation) Grant, No. 387-05/UN7.P4.3/PP/2018. The authors fully acknowledged Institute for Research and Community Services (LPPM) Diponegoro University for the approved fund which makes this important research viable and effective.

References

- [1] K. Gururajan and J. Prakash, Roughness effects in narrow porous journal bearing with arbitrary porous wall thickness, *International Journal of Mechanical Sciences*, 44 (5) (2002) 1003-1016.
- [2] N. B. Naduvanamani, P. S. Hiremath and G. Gurubasavaraj, Effects of surface roughness on the static characteristics of rotor bearings with couple stress fluids, *Computer & Structures*, 80 (2002) 1243-1253.
- [3] G. K. Kalavathi, P. A. Dinesh and K. Gururajan, Influence of roughness on porous finite journal bearing with heterogeneous slip/no-slip surface, *Tribology International*, 102 (2016) 174-181.

- [4] S. Cui, L. Gu, M. Fillon, L. Wang and C. Zhang, The effects of surface roughness on the transient characteristics of hydrodynamic cylindrical bearings during startup, *Tribology International*, 128 (2018) 421–428.
- [5] H. Liu, H. Xu, P. J. Ellison and Z. Jin, Application of computational fluid dynamics and fluid-structure interaction method to the lubrication study of a rotor-bearing system, *Tribology Letters*, 38 (3) (2010) 325–336.
- [6] A. Charitopoulos, D. Fouflias, C. I. Papadopoulos, L. Kaiktsis and M. Fillon, Thermohydrodynamic analysis of a textured sector-pad thrust bearing: Effects on mechanical deformations, *Mechanics & Industry*, 15 (5) (2014) 403–411.
- [7] M. Wodtke, A. Schubert, M. Fillon, M. Wasilczuk and P. Pajaczowski, Large hydrodynamic thrust bearing: Comparison of the calculations and measurements, *Proceedings of the Institution of Mechanical Engineers, Part J: Journal of Engineering Tribology*, 228 (9) (2014) 974–983.
- [8] A. Linjamaa, A. Lehtovaara, R. Larsson, M. Kallio and S. Söchtting, Modelling and analysis of elastic and thermal deformations of a hybrid journal bearing, *Tribology International*, 118 (2018) 451–457.
- [9] T. Adams, C. Grant and H. Watson, A Simple algorithm to relate measured surface roughness to equivalent sand-grain roughness, *International Journal of Mechanical Engineering and Mechatronics*, 1 (2) (2012) 66–71.
- [10] H. K. Versteeg and W. Malalasekera, *An Introduction to Computational Fluid Dynamics, The Finite Volume Method*, Second Ed., Pearson Education Limited, England (2007).
- [11] ANSYS, *ANSYS Fluent, Version 16.0: User Manual*, ANSYS, Inc., Canonsburg, USA (2017).
- [12] S. Cupillard, S. Glavatskih and M. J. Cervantes, Computational fluid dynamics analysis of a journal bearing with surface texturing, *Proceedings of the Institution of Mechanical Engineers, Part J: Journal of Engineering Tribology*, 222 (2) (2008) 97–107.
- [13] G. Gao, Z. Yin, D. Jiang and X. Zhang, Numerical analysis of plain journal bearing under hydrodynamic lubrication by water, *Tribology International*, 75 (2014) 31–38.
- [14] Q. Lin, Z. Wei, N. Wang and Y. Zhang, Effect of recess configuration on the performances of high-speed hybrid journal bearing, *Industrial Lubrication and Tribology*, 68 (3) (2016) 301–307.
- [15] D. Y. Dhande and D. W. Pande, Multiphase flow analysis of hydrodynamic journal bearing using CFD coupled fluid structure interaction considering cavitation, *Journal of King Saud University - Engineering Sciences*, 30 (4) (2018) 345–354.
- [16] D. Sun, S. Li, C. Fei, Y. Ai and R. P. Liem, Investigation of the effect of cavitation and journal whirl on static and dynamic characteristics of journal bearing, *Journal of Mechanical Science and Technology*, 33 (1) (2019) 77–86.
- [17] P. Zwart, A. G. Gerber and T. Belamri, A two-phase flow model for predicting cavitation dynamics, *Proceedings of the Fifth International Conference on Multiphase Flow*, Yokohama, Japan, May (2004).
- [18] B. Jakobsson and L. Floberg, *The Finite Journal Bearing, Considering Vaporization*, Göteborg Gumperts Förlag, Sweden (1957).



10
Mohammad Tauviquirrahman is Head of Laboratory for Engineering Design and Tribology at the Engineering Faculty, Diponegoro University, Indonesia. He received his doctoral degree from Twente University, The Netherlands (2013). His research interests include tribology in lubricant and surface modification.



Jamari is a Senior Researcher at Laboratory for Engineering Design and Tribology at the Engineering Faculty, Diponegoro University, Indonesia. He received his doctoral degree from Twente University, The Netherlands (2006). His research area is contact mechanic and biomechanic.

Influence of roughness on the behavior of three-dimensional journal bearing based on fluid-structure interaction approach

ORIGINALITY REPORT

14%

SIMILARITY INDEX

%

INTERNET SOURCES

14%

PUBLICATIONS

%

STUDENT PAPERS

PRIMARY SOURCES

1

Qiyin Lin, Qingkang Bao, Kejia Li, M.M. Khonsari, Hong Zhao. "An investigation into the transient behavior of journal bearing with surface texture based on fluid-structure interaction approach", Tribology International, 2017

Publication

2%

2

S Cupillard. "Computational fluid dynamics analysis of a journal bearing with surface texturing", Proceedings of the Institution of Mechanical Engineers Part J Journal of Engineering Tribology, 03/01/2008

Publication

2%

3

F.M. Meng, L. Zhang, Y. Liu, T.T. Li. "Effect of compound dimple on tribological performances of journal bearing", Tribology International, 2015

Publication

2%

4

"Proceedings of the 6th International Conference and Exhibition on Sustainable Energy and Advanced Materials", Springer

1%

5

Encyclopedia of Tribology, 2013.

Publication

1 %

6

Hao Zhou, Peitang Wei, Huaiju Liu, Caichao Zhu, Wei Wang. "Crystal elasticity analysis of contact fatigue behavior of a wind turbine gear", Journal of Mechanical Science and Technology, 2019

Publication

1 %

7

Kalavathi, G.K., P.A. Dinesh, and K. Gururajan. "Influence of roughness on porous finite journal bearing with heterogeneous slip/no-slip surface", Tribology International, 2016.

Publication

1 %

8

Nazaruddin Sinaga, Mohammad Tauiviqirrahman, Arif Rahman Hakim, Eflita Yohana. "Effect of Texture Depth on the Hydrodynamic Performance of Lubricated Contact Considering Cavitation", IOP Conference Series: Materials Science and Engineering, 2019

Publication

1 %

9

Xingxin Liang, Zhenglin Liu, Huanjie Wang, Xuhui Zhou, Xincong Zhou. "Hydrodynamic lubrication of partial textured sliding journal bearing based on three-dimensional CFD",

1 %

10

"Design and Development of Broiler Feeding System for Chicken Model Closed-House System", International Journal of Recent Technology and Engineering, 2019

Publication

1%

Exclude quotes

Off

Exclude matches

< 50 words

Exclude bibliography

Off

Influence of roughness on the behavior of three-dimensional journal bearing based on fluid-structure interaction approach

GRADEMARK REPORT

FINAL GRADE

/10

GENERAL COMMENTS

Instructor

PAGE 1

PAGE 2

PAGE 3

PAGE 4

PAGE 5

PAGE 6

PAGE 7

PAGE 8